Optics Communications 86 (1991) 88–92
North-Holland

OPTICS
COMMUNICATIONS

Co-existing attractors in two-photon absorptive optical bistability

N.P. Pettiaux and Paul Mandel
Université Libre de Bruxelles, Campus Plaine C.P. 231, 1050 Brussels, Belgium

Received 27 September 1990; revised manuscript 1 March 1991

We study numerically the branch of periodic solutions that connects the two Hopf bifurcation points of the steady state solution of two-photon absorptive optical bistability. We show that there are two types of hystereses along the branch of periodic solutions. There is one S-shaped hysteresis that ends with a period-doubling cascade leading to chaos. All others hystereses are of the loop-hysteresis type. They contain a small segment of stable periodic solution which bifurcates to chaos either via a Ruelle-Takens route or via a Feigenbaum subharmonic cascade.

Optical bistability (OB) has long been a paradigm for studies of one-photon nonlinear optical process in a passive resonant cavity. It has enjoyed a unique status due to its interest in both fundamental and applied physics [1–3]. In the semiclassical description and in the uniform field limit, absorptive OB is characterized by two stable steady branches connected by an unstable branch. In dispersive OB, on the contrary, both the upper and the lower branches may have Hopf bifurcations leading to self-pulsing and/or chaos. In view of the interest generated by OB, it was quite natural to extend its study by considering the situation in which two photons must be absorbed or emitted when the light beam interacts with the passive two-level medium in the cavity. A semiclassical model for two-photon optical laser amplifier was proposed by Narducci et al. [4] while Arecchi and Politi [5] derived the model for two-photon optical bistability (2OB). From our point of view, the main difference between OB and 2OB is that, even in the absorptive limit, 2OB displays a rich palette of self-pulsing an chaotic solutions. A linear stability analysis of the steady states was published by Ovadia and Sargent [6]. Experimental studies of Doppler-free two-photon interactions in resonant cavities were reported by Giacobino et al. [7], indicating that the system is accessible to experimental scrutiny. Like most two-photon processes, 2OB is phase-sensitive and therefore of interest in studies of squeezed states [8–11a]. Hence absorptive two-photon optical bistability (2AOB) deserves to be studied in more detail.

In two recent papers [12,13], 2OB was shown to belong to a class of models that share the following properties: (i) they involve two-photon processes in resonant cavities; (ii) the steady states become unstable via a Hopf bifurcation of the phases; (iii) in the low-intensity region, there is an hysteresis domain involving two branches of stable periodic solutions. In this work, we wish to complement the analysis reported in ref. [13]. This includes the emergence of the low-intensity hysteresis and the occurrence of additional periodic and chaotic solutions with overlapping domains of existence.

Despite numerous papers published on 2OB, it is surprising to notice that a complete linear stability analysis of the steady states is still lacking. In this communication, we first present a more complete analysis of the steady state linear stability. Then we study the periodic solutions that emerge from the Hopf bifurcations and determine a number of possible coexisting attractors as well as their mechanism of emergence. In particular, we shall show that coexisting attractors (and therefore hystereses) need not be connected by a S-shaped curve but that a "loop-hysteresis" is also a possible mechanism for the coexistence of attractors.

The dynamical equations governing 2AOB are, in scaled variables,

$$X' = \tilde{\kappa}(-X + Y - 2CX^*P) ,$$
$$P' = \tilde{\gamma}_\perp (-P + X^2 F) ,$$
$$F' = -F + 1 - (1/2)[(X^*)^2 P + X^2 P^*] , \quad (1)$$

for the cavity field X, the atomic polarization P and the population difference F. The time has been scaled to the population difference decay rate while $\tilde{\kappa}$ and $\tilde{\gamma}_\perp$ are, respectively, the field and atomic polarization decay rates in units of the population difference decay rate. The input field amplitude is Y which is chosen to be real. Finally C is the usual bistability parameter. In steady state, the relation between the cavity field and the input amplitude is given by

$$Y = X\left(1 + \frac{2C|X|^2}{1+|X|^4}\right). \quad (2)$$

The solution $X = X(Y)$ has a domain of bistability for

$$C \geqslant C_{\text{th}} \equiv 2.71 . \quad (3)$$

The linear stability of the steady solution indicates that when there is a domain of bistability, the branch with a negative slope is always unstable. More important, however, is the result that for

$$C \geqslant C_{\text{H}} \equiv 1 + \gamma^{-1} , \quad \gamma \equiv \tilde{\kappa}/\tilde{\gamma}_\perp , \quad (4)$$

the steady solution is unstable in the domain

$$X_- < |X| < X_+ , \quad X_\pm = [\tilde{C} \pm (\tilde{C}^2 - 1)^{1/2}]^{1/2} ,$$
$$\tilde{C} = C/C_{\text{H}} . \quad (5)$$

Since $0 \leqslant \gamma \leqslant \infty$, we see that $1 \leqslant C_{\text{H}} \leqslant \infty$. Consequently, there can be an instability of the steady solution in the monostable domain. The two points $X_\pm$ are Hopf bifurcations of the phases: if X and P are restricted to be real functions, no instability occurs. The two Hopf bifurcations correspond to the same frequency

$$\Omega^2 = \tilde{\kappa}\tilde{\gamma}_\perp (2 + \tilde{\gamma}_\perp/\tilde{\kappa}) . \quad (6)$$

The above results are not new [11b]. However, what has not been completely studied until now is the position of X_+ and X_- on the bistable curve. Heavy but straightforward algebraic manipulations have shown that the first bifurcation X_- lies necessarily on a part of the lower branch that includes the origin but excludes the limit point. The second bifurcation, at X_+, can be on any of the three branches. More precisely, it can be anywhere on the middle branch, but can access only a finite domain, containing the limit point, of either the upper or the lower branch. Owing to the quartic nature of the equation determining X in steady state, general expressions for the limit point of the lower branch (X_u) and the limit point of the upper branch (X_d) are available but useless. In the limit $C \gg 1$, simple asymptotic expressions have been obtained:

$$X_d = \sqrt{2C}\,[1 - 5/(8C) + O(C^{-2})] ,$$
$$X_u = 3^{1/4}[1 + 2/(C3\sqrt{3}) + O(C^{-2})] ,$$
$$\text{Max}(X_+) = \sqrt{2C}\,[1 - 1/(8C) + O(C^{-2})] ,$$
$$\text{Min}(X_-) = [1 + O(C^{-2})]/\sqrt{2C} . \quad (7)$$

On fig. 1 we display the domains in the parameter plane (γ, C) for which the second Hopf bifurcation is either on the upper branch (upper domain of fig. 1a) or on the lower branch (lower domain of fig. 1b). On fig. 2 we display the positions of the two limit points and the range of variation of the two Hopf bifurcations.

Let us consider now the periodic solutions. Using the software AUTO [14], we have analyzed the periodic solutions that emerge from the Hopf bifurcations of the steady solutions. All numerical calculations were performed for the values

$$\tilde{\kappa} = 1 , \quad \tilde{\gamma}_\perp = 1/2 . \quad (8)$$

The value 1/2 for $\tilde{\gamma}_\perp$ is the radiative limit: it is the smallest possible value that is physically admissible. For these values of the decay rates, the second Hopf

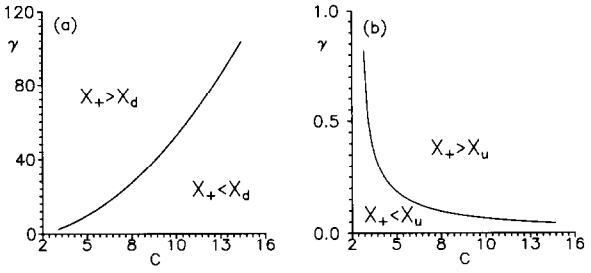

Fig. 1. (a) Domains of parameter space for which the second Hopf bifurcation is on the upper branch ($X_+ > X_d$) or on the middle branch ($X_+ < X_d$). (b) Domains of parameter space for which the second Hopf bifurcation is on the lower branch ($X_+ < X_u$) or on the middle branch ($X_+ > X_u$).

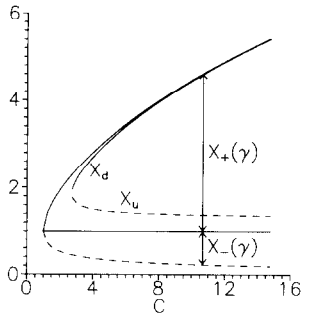

Fig. 2. Range of variation for the first (X_-) and the second (X_+) Hopf bifurcations versus C. For reference, the two limit points of the bistable domain of steady state is also given.

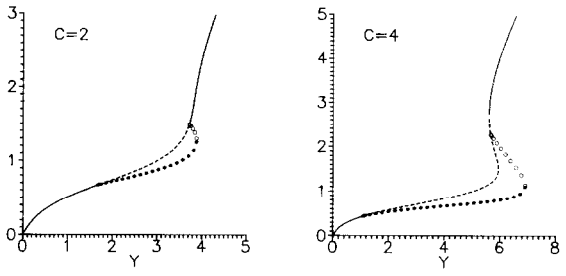

Fig. 3. Instability of monostable ($C=2$) and bistable ($C=4$) steady states. Full lines represent stable steady states. Dashed lines represent unstable steady states. Black circles represent the minimum of Re(X) for stable periodic solutions. Open circles represent the minimum of Re(X) for unstable periodic solutions.

bifurcation at $X=X_+$ is on the intermediate branch with a negative slope when $C>C_{th}$. In all results reported in the following, we find that a continuous branch of periodic solutions connects the two Hopf bifurcations. This branch has segments that are alternately stable and unstable. The first segment, that originates from the first Hopf bifurcation at $X=X_-$, was found to be always stable. The last segment, that connects the periodic solution and the steady state at the second bifurcation point (for $X=X_+$) was found to be always unstable. For the graphical representation of the properties of the periodic solutions, we have determined for each value of C and Y the minimum of the real part of $X(t)$ over a period of oscillation. This minimum was then plotted versus Y. Fig. 3 displays the steady and periodic solutions when C equals 2 and 4. These values were chosen to exemplify a case of instability in the monostable regime ($C=2$) and in the bistable regime ($C=4$). The transition between the stable and unstable periodic solutions occurs at a limit point. We will now describe the transformations of the branch of periodic solutions connecting the two Hopf bifurcations when C is increased. It should be noted, however, that this does not represent all the periodic solutions of eqs. (1), as we shall see.

It was shown in ref. [13] that in the limit $\gamma C\to\infty$ an hysteresis must occur in the branch of periodic solutions. The actual "birth" of this hysteresis domain is captured on fig. 4. It clearly displays how the limit point of the branch of periodic solutions moves in the plane and induces a new pair of periodic solutions contributing to the characteristic S-shaped curve. Since we are plotting the minimum of a periodic function, there is no longer a necessary connection between the slope of the branch and its stability as in the case of steady state solutions. Furthermore, it should be noticed that most of the hysteresis domain observed for $C=7$ overlaps with the domain of stability for the upper steady state branch. Thus there is a domain of coexistence of three stable solutions.

The next modification of the bifurcation diagram is the emergence of a loop in the branch of periodic solutions with a new segment of stable solution as shown on fig. 5 for $C=10$. As C is increased to $C=11$, we observe on fig. 6 the coalescence of two segments of stable periodic solutions corresponding to the disappearence of a very small domain of bistability. On the same figure we also reported, for the sake of completeness, the frequency of the periodic solution versus the pump field amplitude. While we have not seen

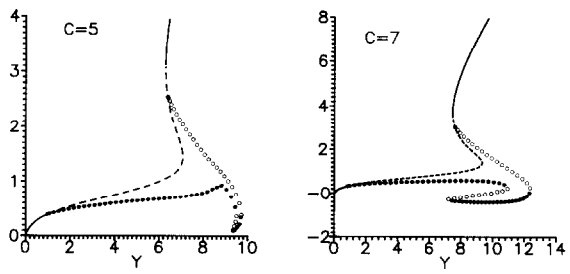

Fig. 4. Emergence of a domain of S-hysteresis by the "motion" of the periodic solution limit point in the plane. Same drawing conventions as in fig. 3.

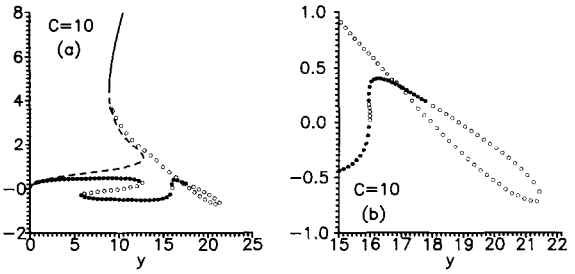

Fig. 5. Emergence of a loop beyond the S-hysteresis. Same drawing conventions as in fig. 3.

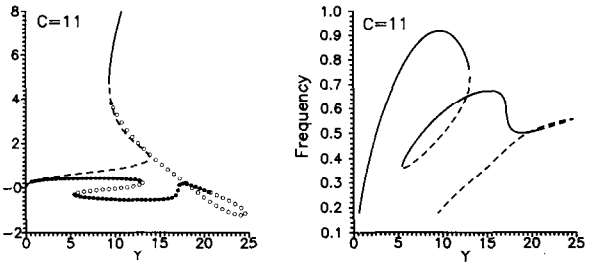

Fig. 6. Final structure of the S-hysteresis. Same drawing conventions as in fig. 3. On the right we show the frequency of the branch of periodic solutions shown on the left.

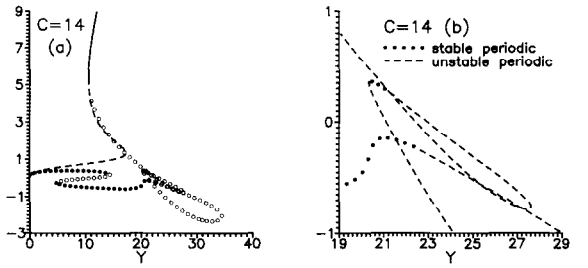

Fig. 7. Emergence of a L-hysteresis. (a) Same drawing conventions as in fig. 3. (b) Focus on the loop.

in the hysteresis other singular points than the limit points, the situation is quite different in the loop where there is a secondary bifurcation point of the stable periodic solution before it reaches the limit point. This secondary bifurcation is a period-doubling bifurcation. It is the first bifurcation of a subharmonic cascade leading to chaos.

The next alteration of the bifurcation diagram is shown on fig. 7. It is the emergence of a second loop in the branch of periodic solutions. This loop is an hysteresis of a different nature. On fig. 8 we have plotted the two types of hystereses for comparison. For the usual hysteresis (or S-hysteresis), the intermediate branch is unstable while the upper and lower branches have a domain of stability. For the loop-hysteresis (or L-hysteresis), it is the upper branch that can be stable while the two lower branches are unstable. This at least would be the situation if we were dealing with a 1D equation, where the slope gives the stability. Still, the generic situation is that two stable branches are connected by an unstable branch in the S-hysteresis while two unstable branches are connected by a stable branch in the L-hysteresis. Fig. 7b focuses on the new L-hysteresis. It shows a small domain of stability. This little segment of stable periodic branch begins at the left limit point and ends with a secondary bifurcation that occurs before the right limit point. At this secondary bifurcation point, a stable quasi-periodic solution (2-torus) emerges. This quasi-periodic solution then bifurcates to chaos. Thus we have a classic Ruelle-Takens route to chaos. For further reference, we shall call L1 a loop-hysteresis where the stable periodic solution begins at the left limit point and bifurcates to chaos via an intermediate quasi-periodic solution (see fig. 9).

When $C=16$, there is no new loop but the nature of the bifurcation diagram has changed. The second loop has still a segment of stable solution, but neither

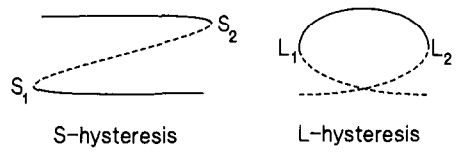

Fig. 8. The two types of hystereses and their limit points.

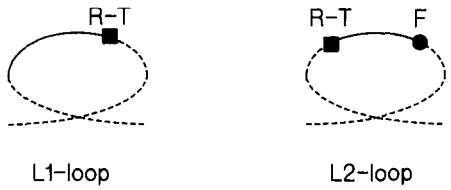

Fig. 9. The two varieties of L-hystereses found in 2AOB. The black square indicates a bifurcation to a quasi-periodic solution followed by a bifurcation to chaos (Ruelle-Takens scenario) when the periodic solution (full line) becomes unstable. The black dot indicates a subharmonic cascade to chaos (Feigenbaum scenario).

does it begin nor does it end at a limit point. Starting from the domain where the periodic solution is stable and increasing the control parameter Y, the stable periodic solution becomes unstable via a period-doubling bifurcation that signals the beginning of a subharmonic cascade to chaos. On the contrary, when we start from the stable periodic branch and decrease the control parameter Y, the instability corresponds to the emergence of a stable quasi-periodic solution which becomes chaotic upon further reduction of Y. Hence the segment of stable periodic solution is the central link in the sequence

$$\text{chaos} \leftarrow \text{2-torus} \leftarrow \text{limit cycle} \rightarrow \text{period-doubling cascade} \rightarrow \text{chaos}. \quad (9)$$

We therefore have the glueing of a direct Feigenbaum cascade and a reverse Ruelle-Takens sequence. We shall refer to that type of L-hysteresis as an L2 loop (see fig. 9).

As C is further increased, additional L-hystereses arise. For $C=18$, a second L-hysteresis exists and for $C=20$ a third L-hysteresis has also been found. We have only analyzed the $C=18$ configuration. The first of these two loops is of the L1 type whereas the second loop is of the L2 type.

This analysis indicates that deep modifications are induced by multiphoton processes, the simplest case of which being the two-photon process. Indeed, in one-photon AOB, there is no Hopf bifurcation at all in the uniform field limit: the only instability is that of the intermediate branch of steady solutions. Another difference between one-photon and two-photon systems is the role played by the dynamical Stark shift (DSS) which is due to the intensity-dependence of the atomic levels. Since the DSS is a second order effect in the field amplitude, it is usually neglected in one-photon processes, but may become important in two-photon processes which are also second order effects in the field amplitude. These shifts introduce a field dependence in the detunings. However, it has been shown [15] that when the atomic transition is not saturated ($F \simeq 1$), the DSS is proportional to $(1-F)^{1/2}$ and may be neglected. We have checked, for the case of fig. 5 (corresponding to $C=10$) that all stable periodic branches are in the domain $F > 3/4$. Furthermore, we have also determined bifurcation diagrams in the nonresonant case, that is, including constant detunings in eqs. (1), and verified that the topology of our bifurcation diagrams is not affected by small detunings. These results suggest that in the parameter domain that we have considered, the DSS will not significantly affect the structure of the bifurcation diagrams. Of course, there is in any case an upper limit of the cavity field X, that depends on the precise energy level configuration, above which the model used in this paper is no longer valid and where the DSS will significantly alter the dynamics of the system.

This work was supported in part by the FNRS (Belgium) and the IAP program of the Belgian government.

References

[1] L.A. Lugiato, Theory of optical bistability, in: Progress in Optics, ed. E. Wolf, Vol. XXI (North-Holland, Amsterdam, 1984) pp. 71–216.
[2] H.M. Gibbs, Optical bistability: controlling light by light (Academic Press, Orlando, 1985).
[3] P. Mandel, S.D. Smith and B.S. Wherret, From optical bistability twoards optical computing (North Holland, Amsterdam, 1987).
[4] L.M. Narducci, W.W. Eidson, P. Furcinitti and D.C. Eteson, Phys. Rev. A 16 (1977) 1665.
[5] F.T. Arecchi and A. Politi, Lett. Nuovo Cimento 23 (1978) 65.
[6] S. Ovadia and M. Sargent III, Optics Comm. 49 (1984) 447.
[7] E. Giacobino, M. Devaud, F. Biraben and G. Grynberg, Phys. Rev. Lett. 45 (1980) 434.
[8] L.A. Lugiato and G. Strini, Optics Comm. 41 (1982) 374.
[9] C.M. Savage and D.F. Walls, Phys. Rev. A 33 (1986) 3282.
[10] B.A. Capron, D.A. Holm and M. Sargent III, Phys. Rev. A 35 (1987) 3388.
[11] (a) O. Galatola, L.A. Lugiato, M. Vadacchino and N.B. Abraham, Optics Comm. 69 (1989) 419; (b) 69 (1989) 414.
[12] L.A. Lugiato, P. Galatola and L.M. Narducci, Optics Comm. 76 (1990) 276.
[13] P. Mandel, N.P. Pettiaux, W. Kaige, P. Galatola and L.A. Lugiato (preprint).
[14] E.J. Doedel, Cong. Num. 30 (1981) 265.
[15] G. Grynberg, B. Cagnac and F. Biraben, in Topics in current physics vol. 21 eds. M.S. Feld and V.S. Letokhov (Springer, Heidelberg, 1980) pp. 111–164.